Application of a semi-microscopic core-particle coupling method to the backbending in odd deformed nuclei

Pavlos Protopapas [*] and Abraham Klein [†]

Department of Physics, University of Pennsylvania, Philadelphia, PA 19104-6396

Niels R. Walet [‡]

Department of Physics, University of Manchester Institute of Science and Technology, P. O. Box 88, Manchester, M60 1QD, United Kingdom

(February 9, 2008)

Abstract

In two previous papers, the Kerman-Klein-Dönau-Frauendorf (KKDF) model was used to study rotational bands of odd deformed nuclei. Here we describe backbending for odd nuclei using the same model. The backbending in the neighboring even nuclei is described by a phenomenological two band model, and this core is then coupled to a large single-particle space, as in our previous work. The results obtained for energies and $M1$ transition rates are compared with experimental data for ^{165}Lu and for energies alone to the experimental data for ^{179}W. For the case of ^{165}Lu comparison is also made with previous theoretical work.

Pacs numbers: 21.60.Ev, 21.10.Re

Typeset using REVTEX

[*]pavlos@walet.physics.upenn.edu

[†]aklein@walet.physics.upenn.edu

[‡]mccsnrw@afs.mcc.ac.uk

I. INTRODUCTION

In two previous applications [1,2], the Kerman-Klein- Dönau-Frauendorf (KKDF) model was used to study rotational bands of selected odd deformed nuclei. In both applications the system was described by an effective interaction which includes a monopole pairing and a quadrupole-quadrupole interaction. In the first application a large single-particle space was coupled to the ground-state band of the neighboring nuclei, whereas in the second application the same large single-particle space was not only coupled to the ground-state band but also to some of the excited bands of the core.

As a second class of applications, we want to describe backbending for odd nuclei using the KKDF model. As has been known for more than two decades, deformed nuclei commonly show a rotational anomaly (known as backbending), where the energetically favored, or yrast, collective band undergoes an abrupt increase in its moment of inertia (as a function of frequency, for example). The generally accepted interpretation is that backbending of an even nucleus occurs when two neutrons (or protons) with high j break their pairing bond and rotationally align perpendicular to the symmetry axis [3]. The rotational-aligned sequence of states is called the s-band. In this application, instead of following a microscopic approach to backbending that incorporates this physics, we have chosen to take a purely phenomenological approach using a model of two coupled bands. These will then be coupled to the extra odd particle in order to achieve a description of the corresponding phenomena in the neighboring odd nuclei. The reason for utilizing a phenomenological description of the even cores is that this provides a more accurate fit to the data than existing microscopic calculations.

In the next section we will present the description of the cores, including the phenomenological model and the results. In Sec. III the results of the energy calculations for ^{179}W will be presented, and in Sec. IV the results for both energies and $M1$ transitions will be given for ^{165}Lu. There is a brief concluding section.

II. CORE PHENOMENOLOGY

In this section we develop a phenomenological description of the backbending phenomenon for the even neighboring nuclei. It is not our purpose to build a complete and sophisticated model but to reproduce the energy levels and the values of the quadrupole matrix elements as accurately as possible, because the results of these calculations will be used as input to the calculations for the odd nuclei. The purpose of the model is simply to provide input data to our theory when experimental values are not sufficiently abundant.

Consider two bands, the ground-state band and an excited band that "cross" at a certain angular momentum I. From experimental observations we know that if such a situation occurs, the bands repel each other (avoided crossing). From the mixture of the bands, we can conclude that the Hamiltonian of the system is in general not axially symmetric, and as a result, the projection K is not a good quantum number. We write the Hamiltonian of such a system as

$$H = H_0 + H_1, \tag{1}$$

where H_0 is the axially symmetric part of Hamiltonian and H_1 is the K quantum number non-conserving Hamiltonian which gives rise to the avoided crossing. The unperturbed Hamiltonian, H_0, describes the ground-state rotational band and one excited band. The excitations in such bands can have the form of the simple rigid rotor, or of the variable moment of inertia model (VMI model) [4,5], or even more general form (see below). For the uncoupled systems, we take the angular momentum I, its projection M, and the projection on the body fixed axis K as good quantum numbers. Therefore, we denote the eigenstates of the unperturbated system as $|IMK\rangle$. Expressed in the unperturbated basis, the Hamiltonian for a given angular momentum will take the following form,

$$H = \frac{\hbar^2}{2} \begin{bmatrix} f_1(\hat{I}^2) & 0 \\ 0 & E_o + f_2(\hat{I}^2) \end{bmatrix} + \begin{bmatrix} 0 & C(\hat{I}) \\ C(\hat{I}) & 0 \end{bmatrix}, \tag{2}$$

where $\hat{I} = I(I + 1)$ and E_o is the bandhead energy. The perturbation has, for the moment, a general $\hat{I}$ dependence. The functions $f_i(\hat{I})$ which describe the angular momentum dependence of the uncoupled band i ($i = 1, 2$) are often represented as a polynomial in $I(I + 1)$,

$$f_i(\hat{I}^2) = \frac{I(I + 1)}{\mathcal{I}_i^0} + \frac{(I(I + 1))^2}{\mathcal{I}_i^1} + \cdots, \tag{3}$$

with expansion coefficients $\mathcal{I}^0$, $\mathcal{I}^1$. This conventional expansion has poor convergence properties at large I. A better expansion of energy as a function of angular momentum is given by the *variable moment of inertia* model (VMI) [6] in which the moment of inertia is a function of angular momentum

$$E(I, \mathcal{I}) = \frac{I(I + 1)}{2\mathcal{I}(I)} + \frac{1}{2} C \left(\mathcal{I}(I) - \mathcal{I}_0 \right)^2, \tag{4}$$

with two parameters C and $\mathcal{I}_0$. The variable moment of inertia $\mathcal{I}(I)$ is determined through use of the variational condition

$$\left. \frac{dE(I)}{d\mathcal{I}(I)} \right|_I = 0. \tag{5}$$

This model can be shown to be equivalent [7] to the two-term approximation to the Harris (cranking) formula [8]. The latter is an expansion of the energy in powers of the "rotational frequency" ω, given by

$$E(\omega) = \mathcal{A}^0 \omega^2 + \mathcal{A}^1 \omega^4 + \mathcal{A}^2 \omega^6 + \cdots, \tag{6}$$

where $\mathcal{A}^0$, $\mathcal{A}^1$ etc are parameters that are fitted to experimental values. Since the concept of continuous angular frequency is not well defined for quantum mechanical systems, the definition used is derived from the corresponding classical definition. In classical mechanics we have,

$$\omega(I) = \frac{dE(I)}{dI}, \tag{7}$$

3

where $E(I)$ is the energy at angular momentum I. In quantum mechanics we take a cue from this definition and choose the discrete definition

$$\omega(I) = \frac{E(I_{+1}) - E(I)}{\hat{I}_{+1} - \hat{I}}, \tag{8}$$

where I_{+1} is the next angular momentum value that the system can take. In our calculations we choose to use the Harris formula to the third order.

At this point we have to specify what form the coupling will take. The exact form of the inter-band interaction is not known. We have chosen to perform the calculations using the standard band coupling formalism [9]. Since the ground state has $K = 0$, the possible cases are limited by the values of K chosen for the excited band. In the following we allow $K = 0, 1$ and 2.

$$\text{For } K = 0 \to K = 1: \qquad C(I) = C\sqrt{I(I+1)}, \tag{9}$$
$$\text{For } K = 0 \to K = 0: \qquad C(I) = CI(I+1), \tag{10}$$
$$\text{Constant interaction}: \qquad C(I) = C. \tag{11}$$
$$\text{For } K = 0 \to K = 2: \qquad C(I) = C(I+1)(I+2)(I-1). \tag{12}$$

The actual angular momentum dependence of the coupling term is not decisive for the following reason: The mixture of two uncoupled band states with the consequent distortion of the shapes of the energies as functions of the angular momentum depends on the strength and the form of the coupling term as well as on the energy difference of the unperturbed states. The bands will be close to each other (in the Energy vrs. J plot) only for a single value of angular momentum, and therefore the mixture will be insignificant for all other values of angular momentum. As soon as the strength of the coupling term is fitted at this angular momentum, the actual functional dependence of the coupling strength becomes irrelevant. For the actual calculations we tried different forms of the coupling and we state in Table I which ones yield the best fit for the nucleus under study.

At this point we have a complete phenomenological description for the backbending phenomena. If we use to the expansion Eq. (6) up to the third order, we then have eight free parameters to fit, namely the six coefficients for the two uncoupled bands, $\mathcal{A}_1^0$, $\mathcal{A}_1^1$, $\mathcal{A}_2^2$, $\mathcal{A}_2^0$, $\mathcal{A}_2^1$ and $\mathcal{A}_2^2$, the band-head energy E_0, and finally the coupling C. This is not a difficult task, and we will describe the details and show the results in the following section.

To calculate the $BE(2)$'s we have to express the matrix elements of the quadrupole operator as a function of the matrix elements in the uncoupled system. To be more specific with the notation, states of the unperturbated Hamiltonian that belong to the ground-state band will be denoted by $|IM0\rangle$ and states that belong the excited band $|IMK\rangle$. For the coupled system states have good angular momentum I, its projection M, but K is not a good quantum number any more. We denote states of the complete system as $|IM1\rangle$ and $|IM2\rangle$. After diagonalizing the Hamiltonian, we can express the eigenstates of the full system as a linear combination of the unperturbed states

$$|IM1\rangle = \lambda_0(I)|IM0\rangle + \lambda_1(I)|IMK\rangle,$$
$$|IM2\rangle = \mu_0(I)|IM0\rangle + \mu_1(I)|IMK\rangle, \tag{13}$$

4

where $\lambda_0(I)$, $\lambda_1(I)$, $\mu_0(I)$ and $\mu_1(I)$ will be provided from the diagonalization of the Hamiltonian. Consequently we can express the matrix elements of the quadrupole operator, in the coupled case, as a function of the matrix elements of the unperturbated case,

$$
\begin{aligned}
\left\langle IM1|\hat{Q}|I'M'1\right\rangle &= \lambda_0(I)\lambda_0(I')\left\langle IM0|\hat{Q}|I'M'0\right\rangle + \lambda_1(I)\lambda_1(I')\left\langle IMK|\hat{Q}|I'M'K\right\rangle \\
&\quad + \lambda_0(I)\lambda_1(I')\left\langle IM0|\hat{Q}|I'M'K\right\rangle + \lambda_1(I)\lambda_0(I')\left\langle IMK|\hat{Q}|I'M'0\right\rangle, \\
\left\langle IM1|\hat{Q}_\mu|I'M'2\right\rangle &= \lambda_0(I)\mu_0(I')\left\langle IM0|\hat{Q}|I'M'0\right\rangle + \lambda_1(I)\mu_1(I')\left\langle IMK|\hat{Q}|I'M'K\right\rangle \\
&\quad + \lambda_0(I)\mu_1(I')\left\langle IM0|\hat{Q}|I'M'K\right\rangle + \lambda_1(I)\mu_0(I')\left\langle IMK|\hat{Q}|I'M'0\right\rangle, \\
\left\langle IM2|\hat{Q}_\mu|I'M'2\right\rangle &= \mu_0(I)\mu_0(I')\left\langle IM0|\hat{Q}|I'M'0\right\rangle + \mu_1(I)\mu_1(I')\left\langle IMK|\hat{Q}|I'M'K\right\rangle \\
&\quad + \mu_0(I)\mu_1(I')\left\langle IM0|\hat{Q}|I'M'K\right\rangle + \mu_1(I)\mu_0(I')\left\langle IMK|\hat{Q}|I'M'0\right\rangle.
\end{aligned}
\tag{14}
$$

The reduced matrix elements of the quadrupole operator $\hat{Q}$ for the uncoupled case are taken from the phenomenological Bohr-Mottelson model,

$$
\left\langle I0 \parallel \hat{Q} \parallel I'K\right\rangle = \sigma_{K'}\, q^{\text{band1}\to\text{band2}}\sqrt{2I+1}\sqrt{2I'+1}\begin{pmatrix} I & I' & 2 \\ 0 & K & -K \end{pmatrix},
\tag{15}
$$

$$
\sigma_{K'} = \begin{cases} \sqrt{2} & K' \neq 0 \\ 1 & K' = 0 \end{cases},
$$

where $q^{\text{band1}\to\text{band2}}$ are the intrinsic quadrupole moments of any inter or intra-band transitions. Consequently we have three more parameters to fit, namely the three intrinsic quadrupole moments. From measured $BE(2)$'s we fix these three parameters and then calculate the rest of the $BE(2)$'s that are needed in the calculation but not available experimentally.

For the first application, ^{179}W, we need the excitation energies and the quadrupole matrix elements of the neighboring even-even nuclei ^{178,180}W. Since we assume particle-number non-conservation the difference between the two neighboring nuclei should be small, and since there are not enough experimental data for ^{178}W, we did the calculations for ^{180}W only. In the special case where the excited band has odd values of angular momentum the fitting can be simplified further. These odd angular momentum states do not interact with the states of the ground state band, and since they belong to the same band, the parameters $\mathcal{A}$ of this band can be calculated independently. First, we fit the parameters $\mathcal{A}_{\text{exc}}^{0,1,2}$ for the states with odd value angular momentum, and then we fit the other 5 parameters. For example the excited band of ^{180}W (see Fig. (1)) has states with odd value I. Therefore, we fitted the upper band first and when the $\mathcal{A}_{\text{exc}}^{0,1,2}$ were found, we fitted the rest. The results are shown in Table (I) along with Fig. (1).

For the $BE(2)$'s we utilize the few experimental data available. As stated above, there are three parameters to fit, q_0, q_K and q_{K0}. With these parameters fixed, we calculated all transitions that will be needed for the calculations of the odd nuclei. The results of the fit are given in Fig. (2) and Table (I).

As a second application we considered the odd proton nucleus ^{165}Lu. The neighboring even nuclei are ^{164}Yb and ^{166}Hf. There are enough experimental values for both these

nuclei, and therefore we have fitted both nuclei and taken the average values of the excitation energies and quadrupole matrix elements for application to the odd nucleus. The calculation was done as described above for ^{180}W with one modification however. We realized that the fitting of the $BE(2)$ values is more sensitive to the strength of the coupling $C(I)$ than are the excitation energies. Therefore, we first do a preliminary fit of the excitations energies. We then adjust the wavefunctions found from these calculations to fit the $BE(2)$ values by allowing C to vary once more, in addition to the necessary choice of intrinsic quadrupole moments. The results are shown in Fig. (4) and in Table (I). Then the excitation energies are re-calculated with an already fixed coupling strength C, and we find new values for the $\mathcal{A}$'s. The results of final fitting of the excitation energies are shown in Fig. (3) and in Table (I).

III. CALCULATIONS AND RESULTS FOR ^{179}W

The equations of motion (EOM), as well as the normalization conditions, for the case of backbending are not formally different from those presented in the two previous applications [1] and therefore will not be repeated. In contrast to these applications, the quadrupole field Γ will not take one of the simplified forms of the Bohr-Mottelson theory, such as Eq. (15). Instead, it will take values that are determined from the calculation described in the previous section, culminating in Eq. (14). The form of Γ is given by,

$$\Gamma_{aIn,cI'n';J} = -\frac{1}{2}\,\kappa(-)^{j_c+I+J}\begin{Bmatrix} j_a & j_c & 2 \\ I' & I & J \end{Bmatrix}\langle In\|Q\|I'n'\rangle,\qquad(16)$$

where $n = 1, 2$, $n' = 1, 2$, and the quadrupole matrix elements, $\langle In\|Q\|I'n'\rangle$, were calculated in the previous section. Notice that Γ depends on the total angular momentum J in contrast to the two previous cases. In the previous calculations, because we assumed axial symmetry, Γ was independent of J. In this application the symmetry is lost, with implications that will be discussed later.

Similarly to the previous two examples, we used a large single-particle space (including all states from 5 major shells). The energies and matrix elements of these single-particle levels were calculated using the Woods-Saxon potential. The core excitations ω_I were taken from calculations for the core described in the previous section. At this point all input parameters are fixed and the only thing remaining to be done is to solve the eigenvalue problem given by the EOM. In the same way as before, the strength of the quadrupole field is treated as a free parameter and the values of the single-particle energies found from Woods-Saxon calculations are allowed to vary by $\pm 5\%$.

Two remaining technical problems should be discussed before we present the results of the calculations. The first difficulty in solving the EOM is that the set of solutions is over-complete by a factor of two, as has previously been discussed. This is a consequence of the fact that the basis states form an over-complete (and, therefore, non-orthogonal set). Consequently half of the states found by solving the EOM are not physical and have to be removed. A technique has been developed to do so and was presented in [1]. In [2], an extension of the technique to the case of avoided crossings, was discussed. In this paper, we summarize only the essential points. The Hamiltonian is first decomposed into

anti-symmetric and symmetric parts with respect to particle-hole conjugation. If only the anti-symmetric part is diagonalized, then for every positive energy eigenvalue there is a negative partner. From the BCS theory we know that the positive eigenvalues are the physical solutions and the negative solutions the non-physical ones. Then the symmetric part was turned on "slowly" and at every step the physical solutions were identified using the projection operator for the physical space built from the wavefunctions of the previous step. The projection operator has an eigenvalue 1 for all real states and 0 for the non-physical states. Since this operator is constructed from wavefunctions of the previous step we expect that it will give an expectation value close to 1 for physical and close to 0 for the non-physical states of the current step. This procedure continues until the symmetric part is turned on fully. In [2], we explained the case where physical and non-physical states of the same angular momentum come very close to each other, and consequently the corresponding wavefunctions change rapidly. In this instance the projection operator method is not valid unless the steps taken are extremely small, making the actual calculation numerically very slow. In this case we utilized the fact that states of the same angular momentum can not actually cross. As stated previously, the two bands involving the near crossing interchange the characters of their wavefunctions as they pass near each other. Since the projection operator method is basically a comparison of wavefunctions, the form of this operator just prior to the crossing would classify a physical state as unphysical and vice versa when used in coarse steps involving the near-crossing. Therefore when this occurs, we adjust the projection operator appropriately in order to make the correct identification in future steps. The problem in now reduced to determining if there is a crossing. This was done by comparing the energy differences between two states at two consecutive steps. This method worked extremely well both in the example of the previous work [1,2] and in the present case.

The second technical problem is the classification of states into different bands. In the first two applications where K was a good quantum number, the identification of bands was done based on the K value of the band. The technique was explained in [1] and again we repeat only essential aspects. In the case that the core is approximated as a rigid rotor, and the formulas of the geometrical model are valid, it turns out that the quadrupole field is independent of the total angular momentum J. This is because of the assumed axial symmetry. As a result when only the antisymmetric part of the Hamiltonian is considered the Hamiltonian has no J dependence. It follows that for a given K, i.e. a given band, all eigenstates with different J are degenerate. We first solve our equation for a minimum possible angular momentum, $J = \frac{1}{2}$. This identifies the $K = \frac{1}{2}$ bands. At $J = \frac{3}{2}$, we find a set of energies equal to those previously found and possibly additional solutions identified as the band heads for $K = \frac{3}{2}$. Continuing in this way we assemble all solutions into a series of flat bands with identified K values.

In the case that backbending occurs, even when the core excitations are neglected (symmetric part of H set to zero) the remaining Hamiltonian is J dependent. Therefore, we can not use the method described above. We can however, take the additional steps of turning off the coupling between the two core bands to return to the axially symmetric case. Then the previous procedure can be used, but there is the additional complication of having to turn on both the symmetric part and the coupling between the two core bands. We can do that in any order, i.e. we can first turn on the coupling between the core bands and then the

core excitation (symmetric part of the Hamiltonian) or the other way around. We choose to do the former. First we turn on the band coupling slowly, and as a result we break the axial symmetry. At every step we compare the wavefunctions at two consecutive steps by calculating the overlap integral. It turns out that even though the J degeneracy is lifted the wavefunctions of the axial and non-axial cases (not including the core excitations) are very similar. Only for a few eigenstates was the mixture between states belonging to different K bands so big we had to turn on the coupling slowly. In most cases large steps were sufficient.

The first application made was to the nucleus ^{179}W. Recent observations [10,11] have been interpreted as showing that for this odd-neutron nucleus, an alignment to an axis intermediate between the deformation axis and the collective rotational axis (Fermi alignment [12]), gives rise to a backbending at $J \sim \frac{31}{2}$. (Frauendorf [12] has called the associated rotational structure a t-band, since the cranking-model description requires a *tilting* of the cranking axis away from the principal axes of the intrinsic prolate spheroidal shape.) Nevertheless we have chosen to try the standard two-band model.

Energy levels of ^{179}W calculated from the present work are presented in Fig. (5). As can be seen from the figure, the yrast band ($K = 7/2$) is reproduced with high accuracy. The same can be said of the first excited band ($K = 7/2$ or tilted-band). Then follow two $K = 1/2$ bands which agree very well with the theory. The most striking feature is the exact reproduction of the staggering nature of the first $K = 1/2$ band. At about 1 MeV above the ground state, theory predicts a $K = 5/2$ band which experimentally is not observed. We believe that this a weakness of the fitting routine for the following reasons. The relative band-head energies were fitted, using a standard fitting routine, to the observed values by varying the strength of the quadrupole field, κ. The fitting was done by minimizing the χ^2. In the absence of an experimental value and the presence of a a theoretical prediction the contribution to the χ^2 is 0. In other words for the fitting routine (at least for the one we used), if the theory predicts a band at low energy that is not observed experimentally it does not increase the χ^2. We are currently working to build a better fitting routine which will be able to avoid such a problem. The result shown in Fig. 5 already represents some improvement over the fitting procedure used initially.

IV. RESULTS FOR ^{165}LU

The second backbending application we tried was to the proton spectra of ^{165}Lu. This nucleus was studied previously by methods related to those of this paper by Chen *et al* [13]. Since it is generally accepted that the s-band in an even nucleus is formed by the decoupling of a pair of quasiparticles from the ground-state band, these authors, among others, decided that it was necessary to use a semi-microscopic description of the backbending in the neighboring even nuclei. However, their fit to the spectra above the backbend leaves something to desired. For this reason, we have chosen to separate the problem of fitting the backbend in the even nuclei from that of fitting the corresponding spectra in the odd nuclei by using a phenomenological two-band mixing model for the even nuclei, which allows, simultaneously an accurate fit to the the spectrum of the crossing bands and to all observed B(E2) values (see previous section). In Fig. (6), we compare our fit for both negative and positive signature ($\alpha = -\frac{1}{2}$, $\alpha = \frac{1}{2}$) crossed bands in ^{165}Lu with those of Chen. The closeness of our fit

compared to that of the previous authors appears simply to reflect corresponding deviations in the spectra of the even neighbors.

We next study magnetic transitions of the yrast band and compare the result to experiment and other theories. In [1] we have presented the equations for the $M1$ matrix element and calculations for the $B(M1)$ transitions of the ground state band of ^{155,157}Gd. To calculate $B(M1)$ rates, we must first evaluate the matrix element of the $M1$ operator between states of the even neighboring cores $\langle I\|M\|I\rangle$ and the matrix elements of the same operator between single particle states (m_{ac}). In the case of $\langle I\|M\|I\rangle$, and because of the limitation on the availability of the experimental data, we have chosen to use a phenomenological model for the value of g, that is derived in [14], namely

$$g = g_R + (g_j - g_R)\,i/I,\tag{17}$$

where g_R refers to the ground band, i is the aligned angular momentum, and g_j is the single particle g factor for the j shell in which alignment occurs. For the $\nu_{13/2}$ level, g_j takes the value of -0.20 and $g_R = 0.31$. In Fig. 7 we show the g factors for the yrast band of ^{166}Hf obtained from the cranking model, the two-quasiparticle plus rotor model, and from the simple formula shown above. For the single particle matrix elements we used a simple formula from [15], Eq. (44) of [1].

Results from different calculations of $B(M1)$ rates of the yrast band of ^{165}Lu are summarized in Fig. 8. Figure 8 shows experimental values from [16], the result from the cranking calculation of [13], a core-particle coupling model also presented in [13] and finally our calculations. Our work reproduces the experimental values quite well and clearly better than the other works.

V. CONCLUSIONS

In this paper we have presented yet another distinct application of the KKDF model. Calculations for ^{165}Lu and ^{179}W were performed starting from a phenomenological description of the neighboring even nuclei. The results are sufficiently satisfactory to encourage us to consider still more sophisticated applications of the model utilized. A fundamental approximation that all applications so far shared was that the incorporation of particle-number conservation into the equations has little effect on the results, because the properties of the neighboring nuclei are so smooth and slowly-varying with particle number. It therefore behooves us to study a case where the incorporation of exact number conservation is essential because we are in a transitional region. Such an has been worked out [17].

ACKNOWLEDGMENTS

REFERENCES

[1] P. Protopapas, A. Klein, and N. R. Walet, Phys. Rev. **C 50**, 245 (1994).

[2] P. Protopapas, A. Klein, and N. R. Walet, Phys. Rev. **C** (in press).

[3] F. S. Stephens, Rev. Mod. Phys. **47**, 43 (1975).

[4] M. A. J. Mariscotti et al., Phys. Rev. **178**, 1864 (1969).

[5] M. A. J. Mariscotti et al., Phys. Rev. **178**, 1864 (1969).

[6] M. A. J. Mariscotti, G. Sharff-Goldhaber, and B. Buck, Phys. Lett. **33B**, 333 (1970).

[7] A. Klein, R. M. Dreizler, and T. K. Das, Phys. Lett. **31B**, 333 (1970).

[8] S. M. Harris, Phys. Rev. **B 509**, 103 (1965).

[9] A. Bohr and B. R. Mottelson, *Nuclear Structure Vol.2*, Benjamin, New York, 1975.

[10] P. M. Walker et al., Phys. Rev. Lett. **67**, 433 (1991).

[11] P. M. Walker and et al, Phys. Lett. **309B**, 17 (1993).

[12] S. Frauendorf, Phys. Scr. **24**, 349 (1981).

[13] Y. S. Chen, P. B. Semmes, and G. A. Leander, Phys. Rev. **C 34**, 1935 (1986).

[14] S. Frauendorf, Physics Letters **100B**, 219 (1981).

[15] P. Ring and P. Shuck, *The Nuclear Many Body Problem*, Springer, Berlin, 1980.

[16] S. Jonsson et al., Nucl. Phys. **A422**, 397 (1984).

[17] P. Protopapas, Ph D thesis, U. of Pennsylvania, 1995.

nucleus	$\mathcal{A}^1_{\text{gs}}$ $\left[\frac{\hbar^2}{keV}\right]$	$\mathcal{A}^2_{\text{gs}}$ $\left[\frac{\hbar^4}{keV^3}\right]$	$\mathcal{A}^3_{\text{gs}}$ $\left[\frac{\hbar^6}{keV^5}\right]$	$\mathcal{A}^1_{\text{exc}}$ $\left[\frac{\hbar^2}{keV}\right]$	$\mathcal{A}^2_{\text{exc}}$ $\left[\frac{\hbar^4}{keV^3}\right]$	$\mathcal{A}^3_{\text{exc}}$ $\left[\frac{\hbar^6}{keV^5}\right]$	Band-Head $[keV]$
^{180}W	17.16	-2.19 10^{-2}	1.95 10^{-5}	6.45	4.00 10^{-3}	1.7 10^{-6}	1663.50
^{164}Yb	18.79	-2.56 10^{-2}	2.10 10^{-5}	6.03	2.21 10^{-3}	2.10 10^{-5}	1603.34
^{166}Hf	20.55	-2.62 10^{-2}	1.90 10^{-5}	6.10	-2.62 10^2	1.92 10^{-5}	1675.34

nucleus	q_0 $[b^2]$	q_K $[b^2]$	q_{0K} $[b^2]$	Coupling Type $[keV]$	Coupling $[keV]$
^{180}W	0.711	0.031	0.66	$C(I) = C\,(I+1)(I+2)(I-1)$	4.21 10^{-5}
^{164}Yb	0.540	0.021	0.41	$C(I) = C\,I\,(I+1)$	1.30 10^{-1}
^{166}Hf	0.560	0.019	0.39	$C(I) = C\,I\,(I+1)$	1.37 10^{-1}

TABLE I. Values obtained for the parameters for the phenomenological model of the even cores. The subscribe "exc" on $\mathcal{A}_{\text{exc}}$ identifies the values of the excited bands.
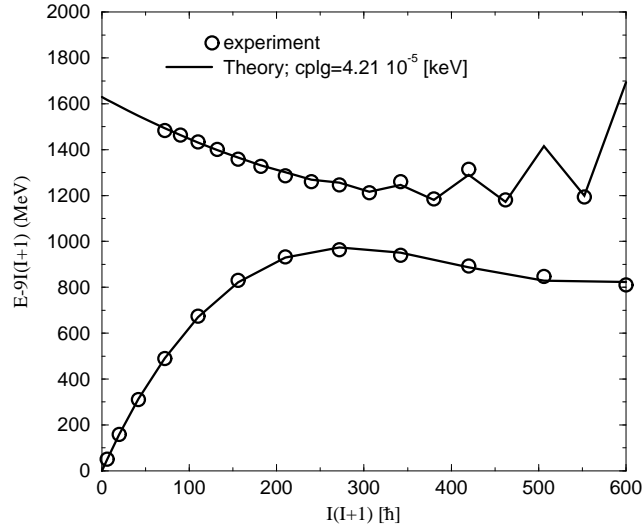
^{180}W

FIG. 1. Fit of the ground-state band and the first excited band of ^{180}W to a phenomenological two-band model. Solid lines represent the theoretical values with coupling equal to 4.3 10^{-5}keV. The experimental values are represented by circles.
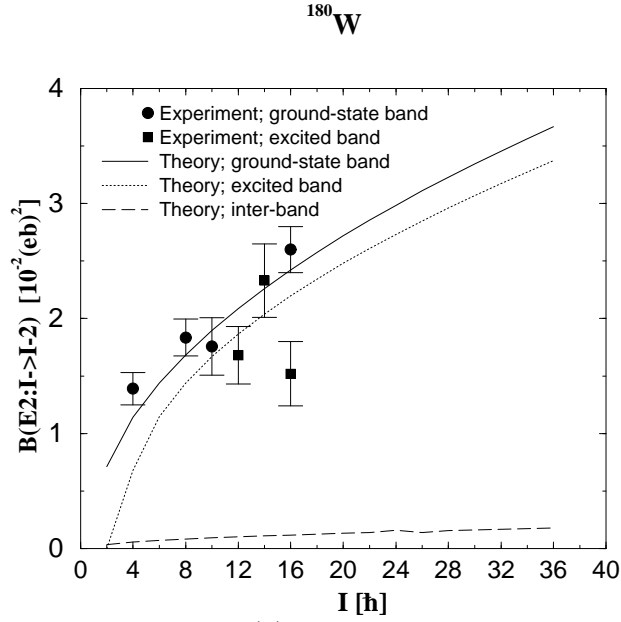
^{180}**W**

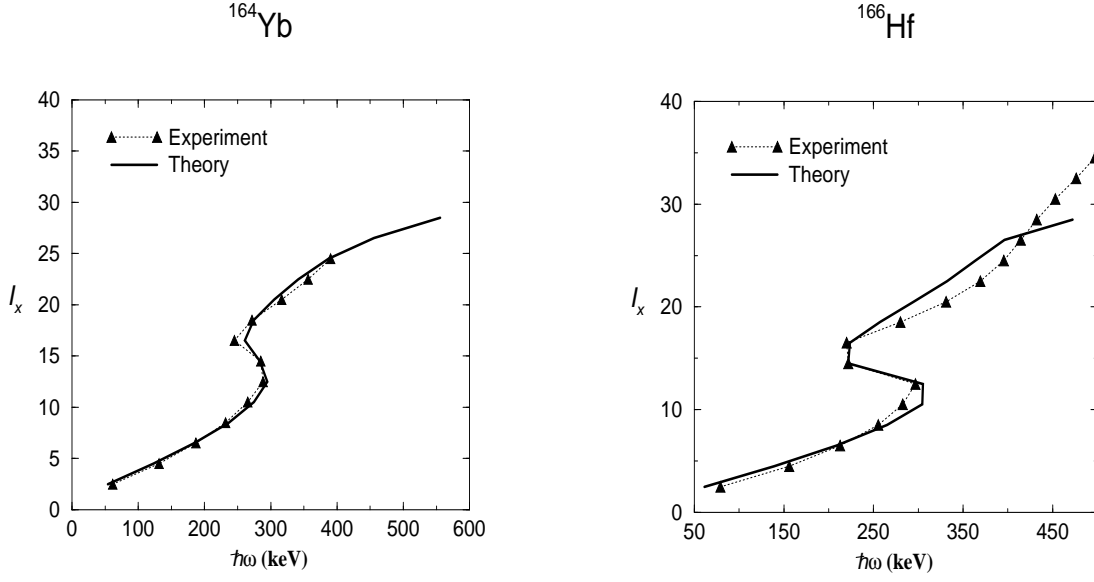FIG. 2. Experimental and theoretical $BE(2)$ values for the yrast band and first excited band.

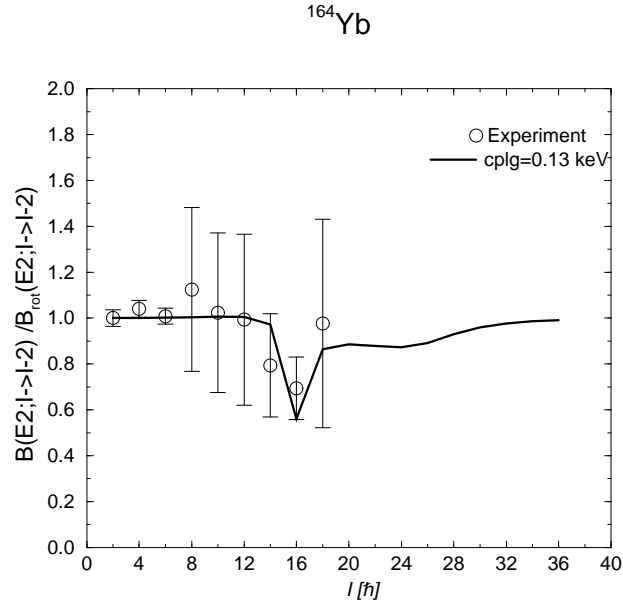FIG. 3. Energy levels of ^{164}Yb (left) and ^{166}Hf (right). Both experiment and theory are shown.

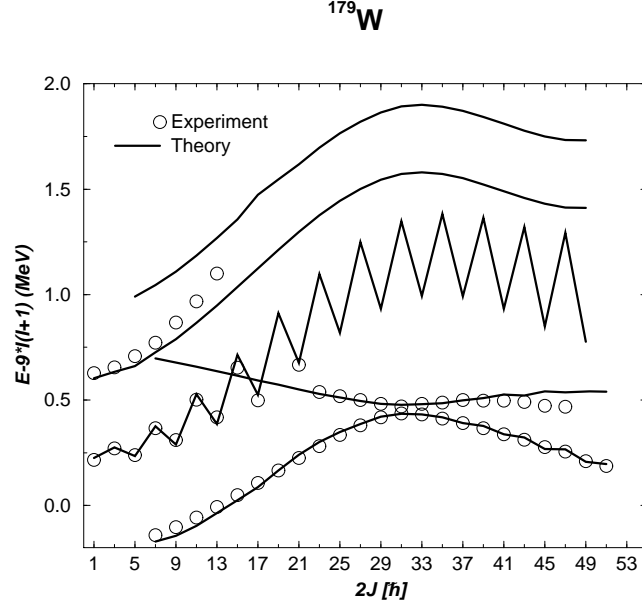FIG. 4. $BE(2)$ values from experiment (circles) and theoretical fit (solid line) of ^{164}Yb.

179W

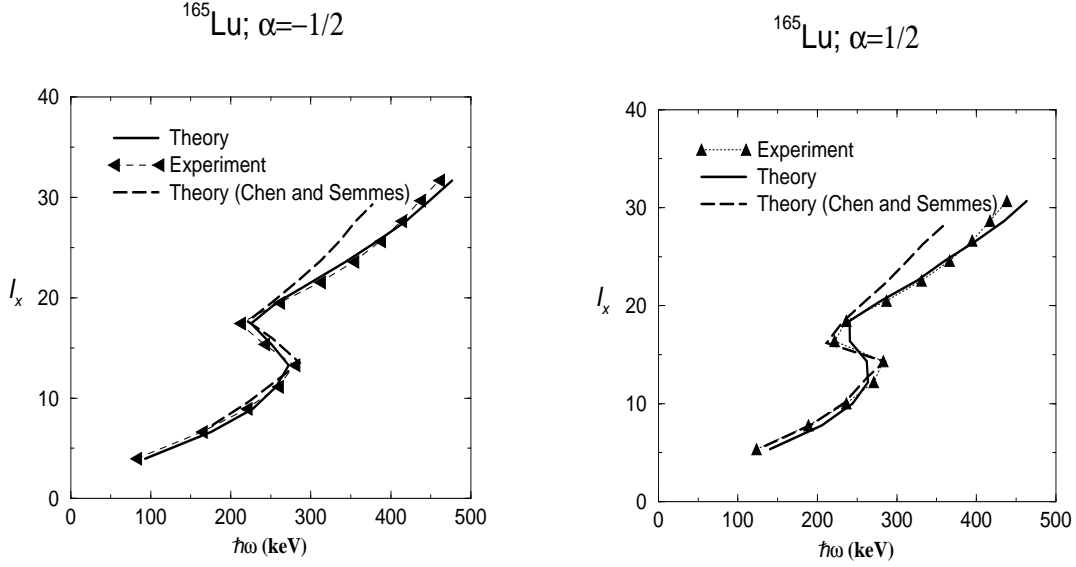FIG. 5.   Comparison of theoretical results to observed energy levels of ^{179}W.

FIG. 6.   Comparison of the observed yrast band of ^{165}Lu with theory. On the left are the negative signature states ($\alpha = -\frac{1}{2}$) and on the right are the positive signature states ($\alpha = \frac{1}{2}$).
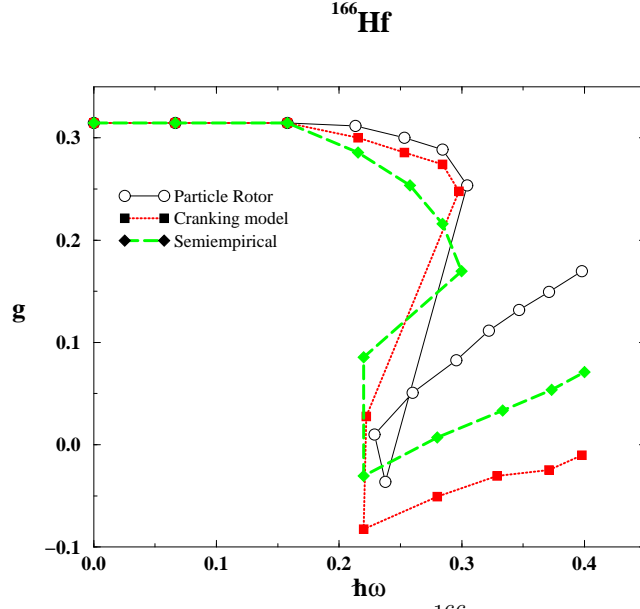
FIG. 7. Calculated g factors for the yrast states of ^{166}Hf. Squares are calculations from the cranking model, the circles are from the two-quasiparticle plus rotor model, and the triangles are from the [14].
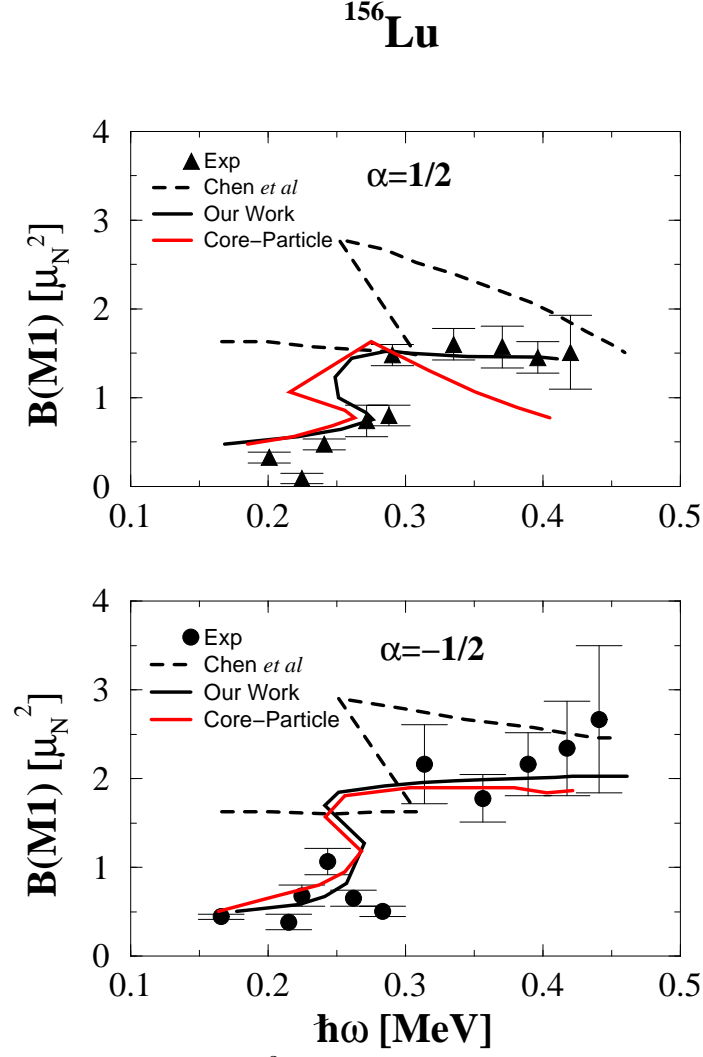
^{156}Lu

FIG. 8. $B(m1)$ transitions rates in μ_N^2. On the top are the positive signature states $(\alpha = -\frac{1}{2})$ and on the bottom are the negative signature states $(\alpha = \frac{1}{2})$. Experimental data [16] are solid symbols, strong coupling model is the chain lines, our work is represented with the solid lines and the work of Chen *et al* [13] is the dashed lines.